

See discussions, stats, and author profiles for this publication at: <https://www.researchgate.net/publication/228754065>

Electrochemical Studies of Langmuir–Blodgett Thin Films of Electroactive Nanoparticles

ARTICLE *in* LANGMUIR · OCTOBER 2001

Impact Factor: 4.46 · DOI: 10.1021/la0107042

CITATIONS

44

READS

24

1 AUTHOR:



Shaowei Chen

University of California, Santa Cruz

218 PUBLICATIONS 7,633 CITATIONS

SEE PROFILE

Electrochemical Studies of Langmuir–Blodgett Thin Films of Electroactive Nanoparticles

Shaowei Chen[†]

Department of Chemistry, Southern Illinois University, Carbondale, Illinois 62901-4409

Received May 10, 2001. In Final Form: July 18, 2001

Thin films (monolayers and multilayers) of ω -ferrocenated gold nanoparticles were fabricated by using the Langmuir–Blodgett technique. The transfer of nanoparticle layers onto a solid substrate surface was quite efficient for the first few layers, exhibiting a proportional increase of optical absorption in the UV–vis range. The interfacial dynamics of the nanoparticle monolayers was studied by using electrochemical methods where the surface reorganization was ascribed to the particle molecular mobility due to relatively weak interparticle interactions. With depositions of more nanoparticle layers, the particle thin films became less conductive, resulting in the anodic shift of the ferrocene formal potential. Because of the compact characteristics of the nanoparticle thin films, not all ferrocene sites were active and accessible, and the corresponding voltammetric currents varied only slightly with more particle layers.

Introduction

The extensive research interest in nanometer-sized particulate materials has been mainly driven by their broad impact on a wide variety of fields,^{1,2} in particular, in the so-called “bottom-up” approach to the miniaturization of optoelectronic devices, chemical and biological sensors, etc.³ One of the technological challenges is to fabricate robust and organized assemblies of these nanoscale building blocks where the collective structural properties and functions might be manipulated by the nature as well as the composition of the nanoparticles. Among the various techniques developed, self-assembling has been quite effective in creating ordered superlattices of nanoparticles by exploiting the molecular interactions such as van der Waals forces, chemisorptive bonding, electrostatic interactions, etc.^{4–6} A key structural element is the bifunctional bridges which link the nanoparticles to the substrate surfaces and/or between layers of nanoparticles, such as aliphatic dithiols. This process can be achieved by using simple beaker chemistry.

Another effective approach is the Langmuir–Blodgett (LB) technique,^{7–9} where a monolayer of nanoparticles is formed on the water subphase surface, and the interparticle spacing and thin film properties can be manipulated

readily with the compression/release of a mechanical barrier. This is one of the advantages as compared to the self-assembling approach. For instance, Heath et al.^{8a} observed an insulator-to-metal transition of Langmuir monolayers of organically functionalized silver nanoparticles by compressing the nanoparticles to an interparticle separation of a mere 5 Å. Recently, we demonstrated that, by introducing additional rigid bifunctional linkers to the air/water interface, large-scale robust and cross-linked nanoparticle networks could be constructed at relatively high surface pressures due to ligand intercalation and the subsequent surface place exchange reactions,⁷ leading to the drastic enhancement of the mechanical stability of the nanoparticle assemblies. These macroscopic-sized nanoparticle patches can then be utilized for surface nanofabrication in a nonlithographic manner.^{7b}

The versatile LB technique should be able to be extended to electroactive nanoparticles as well; however, this subject has not received extensive attention so far. The major motivation comes from the more complicated chemical functionalization of the nanoparticle assemblies. For instance, ferrocene has been used quite extensively as a model system in the investigation of interfacial electron-transfer kinetics. One of the typical approaches is based on immobilizing the ferrocene moieties onto electrode surfaces through an aliphatic chain where the separation of reaction products and the detection of electron-mediation effect might be facilitated. Two-dimensional (2D) self-assembled monolayers of monomeric alkanethiols with ω -ferrocene moieties are among the most extensively studied examples.^{10,11} Nanosized particle-supported ferrocene functional groups represent a novel and yet more complicated three-dimensional system, where, in contrast

[†] E-mail: schen@chem.siu.edu.

(1) See all the review articles in the February 16, 1996 and November 24, 2000 issues of *Science*.

(2) See, for instance: the Special Reports in the October 16, 2000 issue of *Chem. Eng. News*.

(3) (a) Sun, S.; Murray, C. B.; Weller, D.; Folks, L.; Moser, A. *Science* **2000**, *287*, 1989. (b) Kiely, C. J.; Fink, J.; Brust, M.; Bethell, D.; Schiffrin, D. J. *Nature* **1998**, *396*, 444. (c) Wang, Z. L. *Adv. Mater.* **1998**, *10*, 13. (d) Pileni, M.-P. *New J. Chem.* **1998**, 693. (e) Whetten, R. L.; Shifagin, M. N.; Khoury, J. T.; Schaaff, T. G.; Vezmar, I.; Alvarez, M. M.; Wilkinson, A. *Acc. Chem. Res.* **1999**, *32*, 397. (f) Murray, C. B.; Kagan, C. R.; Bawendi, M. G. *Science* **1995**, *270*, 1335. (g) Osifchin, R. G.; Andres, R. P.; Henderson, J. I.; Kubiak, C. P.; Dominey, R. N. *Nanotechnology* **1996**, *7*, 412.

(4) (a) Schmid, G. *J. Chem. Soc., Dalton Trans.* **1998**, 1077. (b) Andres, R. P.; Bielefeld, J. D.; Henderson, J. I.; Janes, D. B.; Kolagunta, V. R.; Kubiak, C. P.; Mahoney, W. J.; Osifchin, R. G. *Science* **1996**, *273*, 1690. (c) Feldheim, D. L.; Grabar, K. C.; Natan, M. J.; Mallouk, T. E. *J. Am. Chem. Soc.* **1996**, *118*, 7640. (d) Taton, T. A.; Mucic, R. C.; Mirkin, C. A.; Letsinger, R. L. *J. Am. Chem. Soc.* **2000**, *122*, 6305. (e) Mann, S.; Shenton, W.; Li, M.; Connolly, S.; Fitzmaurice, D. *Adv. Mater.* **2000**, *12*, 147.

(5) (a) Feldheim, D. L.; Keating, C. D. *Chem. Soc. Rev.* **1998**, *1*, 27. (b) Collier, C. P.; Vossmeier, T.; Heath, J. R. *Annu. Rev. Phys. Chem.* **1998**, *49*, 371.

(6) (a) Chen, S. *J. Phys. Chem. B* **2000**, *104*, 663. (b) Chen, S. *J. Am. Chem. Soc.* **2000**, *122*, 7420.

(7) (a) Chen, S. *Adv. Mater.* **2000**, *12*, 186. (b) Chen, S. *Langmuir* **2001**, *17*, 2878.

(8) (a) Collier, C. P.; Saykally, R. J.; Shiang, J. J.; Henrichs, S. E.; Heath, J. R. *Science* **1997**, *277*, 1278. (b) Heath, J. R.; Knobler, C. M.; Leff, D. V. *J. Phys. Chem. B* **1997**, *101*, 189. (c) Yi, K. C.; Hórvölgyi, Z.; Fendler, J. H. *J. Phys. Chem.* **1994**, *98*, 3872.

(9) Lee, W.-Y.; Hostetler, M. J.; Murray, R. W.; Majda, M. *Isr. J. Chem.* **1997**, *37*, 213.

(10) For instance: (a) Sikes, H. D.; Smalley, J. F.; Dudek, S. P.; Cook, A. R.; Newton, M. D.; Chidsey, C. E. D.; Feldberg, S. W. *Science* **2001**, *291*, 1519. (b) Chidsey, C. E. D.; Bertozzi, C. R.; Putvinski, T. M.; Muijsce, A. M. *J. Am. Chem. Soc.* **1990**, *112*, 4301. (c) Tender, L.; Carter, M. T.; Murray, R. W. *Anal. Chem.* **1994**, *66*, 3173.

(11) (a) Sumner, J. J.; Creager, S. E. *J. Am. Chem. Soc.* **2000**, *122*, 11914. (b) Creager, S. E.; Rowe, G. K. *J. Phys. Chem.* **1994**, *98*, 5500.

to their two-dimensional counterparts,¹² the ferrocene moieties are "concentrated" on the nanoscale particle surface. Previous electrochemical studies¹² of ω -ferrocenated nanoparticles in solutions have shown that the particle-bound ferrocene moieties undergo (independent) successive 1-e redox reactions due to the rapid spinning of the nanoparticles in solutions.

However, when the particles are immobilized onto a substrate surface, due to the three-dimensional (3D) nature of the particle core, the associated interfacial electron transfer between the ferrocene moieties and the electrode might be complicated by the interactions with electrolyte ions (charge compensation, for instance) as well as double-layer effects.¹³ The spatial distribution of the ferrocene moieties on particle surface is anticipated to lead to the variation of the energetic states, demonstrated in different redox (over)potentials. In addition, in multilayer thin films, the electrochemical responses of the electroactive moieties buried within the thin films might be further complicated by ion penetration/compensation as well as charge propagation. Thus, in this report, we describe a series of electrochemical studies of Langmuir thin films of ferrocenated gold nanoparticles, where effects of the particle film thickness on the ferrocene electrochemistry will be investigated. In particular, the electroactive ferrocene moieties will serve as the molecular probe to electrochemically examine the interfacial dynamics of the MPC surface thin films.

Experimental Section

Materials Preparation. All chemicals and solvents (Fisher/ACROS) were used as received except for potassium nitrate (KNO_3) which was recrystallized twice prior to use. Water was supplied with a Barnstead Nanopure water system (18.3 M Ω). Gold nanoparticles (diameter ~ 2 nm, characterized by transmission electron microscopic measurements) protected with a monolayer of *n*-octanethiolates (C8Au MPCs) were synthesized by following a literature route.¹⁴ Multiple copies of 8-mercaptoctylferrocene (HSC8Fc) were incorporated into the particle protecting monolayer by using ligand place-exchange reactions with the resulting nanoparticles denoted C8FcAu.¹² The final surface concentration was found to be approximately 5%, corresponding to average 4.6 Fc moieties per particle as characterized by proton nuclear magnetic resonance (^1H NMR) measurements. Gold thin films were prepared by vapor-depositing ca. 200 nm of gold onto cleaned microscope glass slides.

Fabrications of Particle Surface Layers. The particle surface layered structures were constructed by using the Langmuir–Blodgett technique with a NIMA 611D LB trough. A particle solution of 1.75 mg/mL (ca. 23 μM) was prepared by dissolving the particles in hexane, typically 50–70 μL of which was spread dropwise onto the water surface with a Hamilton microliter syringe. At least 20 min was allowed for solvent evaporation before the first compression isotherm was acquired. The time interval between consecutive compression cycles was also kept at least 20 min. The compressing rate was 20 cm^2/min , and during deposition of particles onto the substrates the lifting speed was maintained at 1 mm/min. Here two types of substrates were used; for electrochemical measurements, gold thin films supported on microscope glass slides were used while for optical measurements plain microscope glass slides (Fisher) were used instead. Both the gold films and glass slides were subjected to ultraviolet-ozone cleaning (Jelight UVO cleaner model 42) for 15 min prior to particle deposition.

Spectroscopic Measurements. ^1H NMR spectroscopy was carried out with a Varian 300 VX NMR spectrometer with

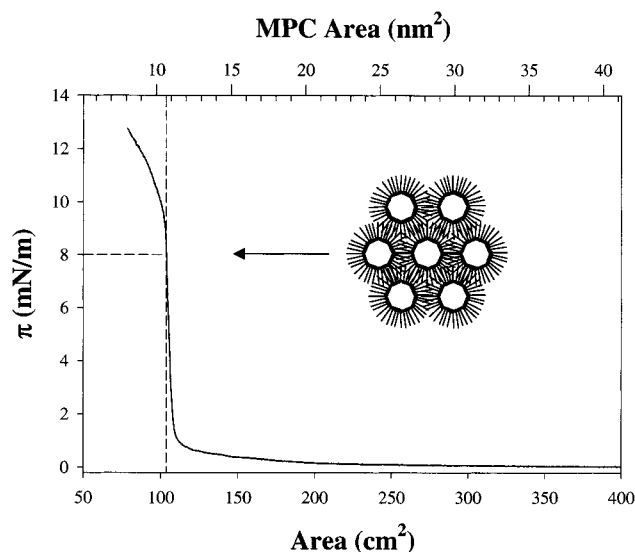


Figure 1. Langmuir isotherm of C8FcAu particles on water surface. 70 μL of 1.75 mg/mL particle solution was spread onto the water surface. Compression rate 20 cm^2/min . Dash lines depict the deposition pressure and surface area. Inset shows a schematic of the structure of the nanoparticle assemblies on the water surface.

concentrated particle solutions prepared in benzene- d_6 , where the absence of sharp peaks indicated the samples were spectroscopically clean (of free ligands). In addition, the peak areas of the methyl and ferrocenyl moieties were used to calculate the surface concentration of ferrocenated ligands after exchange reactions. UV–vis spectroscopy was performed with an ATI Unicam (UV4) UV–vis spectrometer with a resolution of 2 nm. A blank glass slide was used as the reference.

Electrochemical Measurements. Electrochemical measurements were carried out with a BAS 100B/W electrochemical workstation. The gold thin films (with deposited particle layers) were used as the working electrode, a Ag/AgCl (3 M NaCl, from BAS) as the reference, and a Pt coil as the counter electrode. The electrolyte solution (0.10 M KNO_3) was deaerated for at least 20 min with a water-saturated N_2 stream and blanketed with a N_2 atmosphere during the entire experimental process.

Results and Discussion

We begin with an investigation of the phase behaviors of the particles on the water surface, followed by optical and electrochemical studies of the particle assemblies deposited by using the Langmuir–Blodgett technique. Effects of the thickness of particle layers will be investigated. The interfacial dynamics of the MPC thin films deposited onto electrode surfaces will also be discussed.

Langmuir Thin Films. Figure 1 shows a representative surface pressure (π)–area (A) isotherm of the above C8FcAu nanoparticles on a water surface, which is quite similar to those observed with simple alkanethiolate-protected gold nanoparticles.⁷ One can see that, at surface area greater than 12 nm^2/MPC , the surface pressure is virtually zero, indicating a two-dimensional gaseous phase of the particles on the water surface. However, at area smaller than 12 nm^2/MPC , the surface pressure starts to increase drastically, where the steep rising slope suggests the rigid nature of particle close-packed thin films. By assuming a hexagonal distribution of the particles in the thin films (Figure 1, inset), this takeoff area (12 nm^2/MPC) corresponds to a center-to-center distance of about 3.72 nm. As the fully extended chain length of an octanethiolate is 1.01 nm (calculated by Hyperchem), this distance is somewhat smaller than the nanoparticle molecular diameter (core + two monolayer ligands),

(12) (a) Hostetler, M. J.; Green, S. J.; Stokes, J. J.; Murray, R. W. *J. Am. Chem. Soc.* **1998**, *118*, 4212. (b) Green, S. J.; Stokes, J. J.; Hostetler, M. J.; Pietron, J. J.; Murray, R. W. *J. Phys. Chem. B* **1997**, *101*, 2663.

(13) Smith, C. P.; White, H. S. *Anal. Chem.* **1992**, *64*, 2398.

(14) (a) Brust, M.; Walker, M.; Bethell, D.; Schiffrin, D. J.; Whyman, R. *J. Chem. Soc., Chem. Commun.* **1994**, 801. (b) Templeton, A. C.; Wuelfing, W. P.; Murray, R. W. *Acc. Chem. Res.* **2000**, *33*, 27.

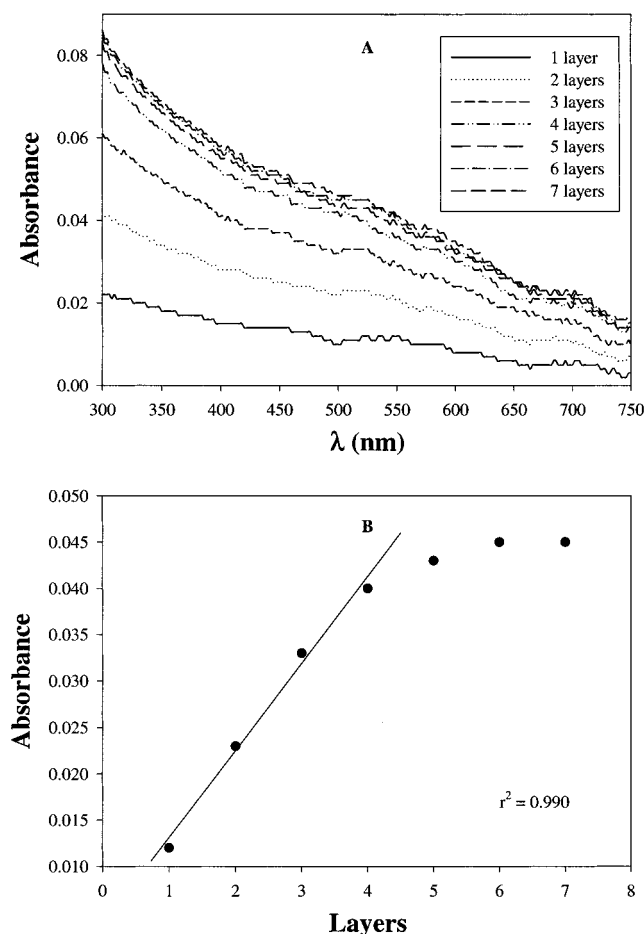


Figure 2. (A) UV-vis spectra of varied layers of C8FcAu particles deposited at 8 mN/m onto a microscope glass slide. A blank glass slide was used as the reference. (B) Variation of absorbance (at 520 nm) with the number of particle layers.

indicating the initiation of ligand intercalation at this surface area, leading to the observed sharp increase in surface pressure with further compression.

A second transition starts at 10.5 nm²/MPC, with a somewhat smaller rising slope. This might be ascribed to the further ligand intercalation between neighboring particles leading to the formation of solidlike close-packed MPC thin films on the water surface. In fact, on the water surface, brown MPC thin films are very visible.

The particle monolayers were then deposited onto a glass slide using the Langmuir-Blodgett (LB) technique (vertical deposition) at $\pi = 8$ mN/m with a lifting speed of 1 mm/min. Figure 2A shows the optical responses of the resulting particle LB assemblies. While the surface plasmon band of nanosized gold particles is not very well-defined here, partly due to the small particle core size (ca. 2 nm in diameter), the absorption profiles do exhibit a Mie character, where the absorption intensity decreases exponentially with decreasing photon energy. In addition, the absorption intensity at 520 nm (the surface plasmon band position of alkanethiolate-protected gold nanoparticles¹⁴) shows a linear increase with the thickness of nanoparticle layers up to four monolayers (Figure 2B), indicating a rather repeatable and efficient transfer of the nanoparticle thin films. This is similar to the observation with self-assembled nanoparticle thin films fabricated by alternating layers of nanoparticles and dithiol linkers.¹⁵ However, further deposition appears to be less efficient, and the corresponding optical absorbance of the particle assemblies starts to level off.

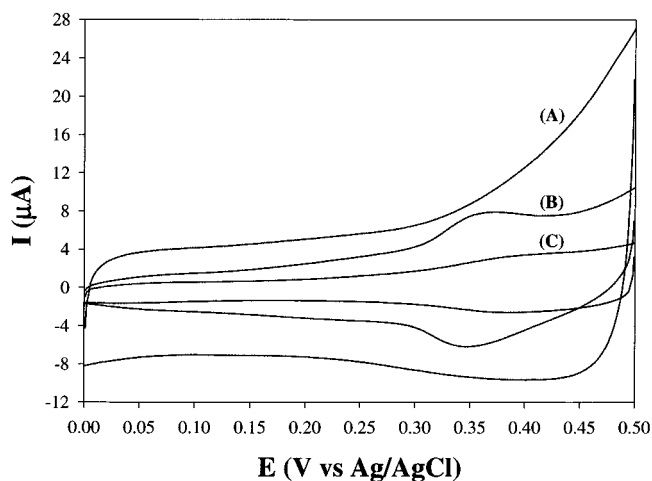


Figure 3. Cyclic voltammograms of (A) a naked gold thin film electrode (0.48 cm²), (B) with a C8FcAu particle monolayer freshly deposited at 8 mN/m, and (C) with the same MPC monolayer after about 20 min in 0.10 M KNO₃. Potential sweep rate 100 mV/s.

Interfacial Dynamics. As the MPC molecules in these LB thin films are not chemically cross-linked to each other, the particles might exhibit some degrees of mobility when deposited onto the substrate surface, though not as free as in solution.^{7b} This could lead to particle reorganization (i.e., annealing) and be monitored by electrochemical measurements using the electroactive ferrocene moieties as the molecular probes. Figure 3 shows the cyclic voltammogram of a C8FcAu particle monolayer (B) freshly deposited onto a gold thin film electrode in 0.10 M KNO₃. One can see that compared to that at the same bare electrode (A) the charging current within the potential range of 0 to +0.5 V is suppressed substantially, indicating the coating of organically functionalized gold MPCs onto the electrode surface. In addition, a pair of voltammetric peaks are observed at +0.36 V with a peak splitting of only 20 mV, suggesting a very facile electron-transfer reaction. These peaks are ascribed to the oxidation/reduction of the particle-bound ferrocene moieties, where the peak currents are found to increase linearly with potential sweep rate (Figure 4), consistent with a surface-confined system. From the slope (Figure 4B), one can estimate the effective surface coverage of ferrocene moieties as $\Gamma_{Fc} = 3.87 \times 10^{13}$ molecules/cm²; hence, the MPC surface coverage (Γ_{MPC}) is 8.41×10^{12} particles/cm², corresponding to an effective particle area of 11.9 nm², somewhat larger than the original MPC area during LB deposition (10.7 nm², Figure 1). This might be accounted for by at least two possibilities; e.g., MPC molecular area expanded due to interfacial dynamics (relaxation), and/or part of the MPC-supported ferrocene moieties were not accessible and active (vide infra).

Additionally, this ferrocene surface concentration corresponds to 20% of the approximate maximum coverage of α -mercaptoalkyl ferrocene derivatives self-assembled onto flat gold surfaces.^{10,11} The appearance of a single pair of voltammetric waves for the ferrocene sites in the LB monolayers suggests a similarity of the energetic states of these surface electroactive groups. In our earlier (unpublished) studies where a compact monolayer of ω -ferrocenated particles was formed by chemisorptive linkages to the electrode surface (particles were first rendered surface active with peripheral thiol groups by

(15) Brust, M.; Bethell, D.; Kiely, C. J.; Schiffrin, D. J. *Langmuir* 1998, 14, 5425.

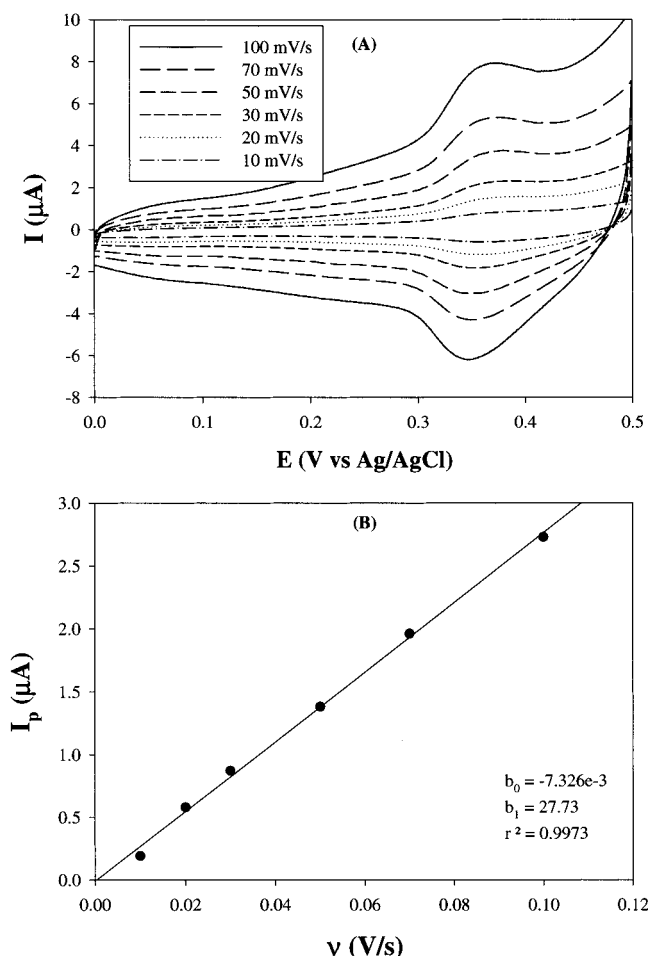


Figure 4. (A) Cyclic voltammograms of the freshly deposited C8FcAu MPC monolayer (as in Figure 3B) in 0.10 M KNO_3 at various potential sweep rates. (B) Variation of the voltammetric peak currents with potential scan rate. Line is the linear regression.

incorporating multiple copies of alkanedithiols into the particle protecting monolayer through exchange reactions⁶), the resulting electrochemical measurements revealed two pairs of voltammetric waves which were ascribed to the variation of ferrocene energetic states due to spatial distribution on the particle surface.¹⁶ Similar phenomena were also reported with two-dimensional mixed monolayers of ω -ferrocenated alkanethiols and n -alkanethiol derivatives at relatively high ferrocene surface coverage.^{10,11} There appear to be at least two possibilities to account for the discrepancy observed here. First, it might be attributed to the fact that the LB-deposited particle molecules might still possess some degree of conformational mobility, in part, because the interactions between the particles and between the particles and the electrode surface mainly involved weak van der Waals forces,^{7b} as compared to the chemisorptive interactions by thiols on gold in the self-assembled systems.^{10,11} Despite the fact that the particle layers were deposited at relatively high surface pressures (e.g., 8 mN/m), not all particles appeared to be in the crystalline configuration, i.e., intercalated to each other, due to

particle size dispersity.^{7a} Thus, in this case, part of the particle assemblies might be free to rotate on the electrode surface (though unlikely to desorb from the electrode surface), which might then help initiate the interfacial dynamic transition of the MPC monolayers, rendering the ferrocene sites accessible to the electrode electron. A second possibility is that the initial LB thin film might possess some defects which facilitate ion transport for charge compensation during the electrooxidation/reduction of the ferrocene groups (more discussion below).

The dynamic characters of the electrode-supported particle assemblies were further observed voltammetrically. Figure 3C shows the cyclic voltammogram of the above same particle monolayer assemblies after ca. 20 min of potential sweeps. Compared to that observed with a freshly deposited MPC monolayer (B), there are two aspects that warrant attention here. First, the interfacial charging current (within 0 to +0.3 V) actually decreases upon the aging of the monolayer, suggesting some surface rearrangement of the deposited particle molecules. This is akin to potential-induced annealing. The driving force of these particle rearrangements seems likely to originate from the bulky ferrocene sites, which, when oxidized (to positively charged ferrocenium), became energetically less favorable to stay in a hydrophobic environment and hence less likely to have an interpenetration conformation with the monolayer ligands of neighboring particles. This deintercalation leads to the more spread-out of MPC molecules and enhances hydrophobic interactions between the surface particle molecules, consequently decreasing the double-layer charging current (by reducing the electrode surface defect sites, for instance). This is also consistent with the above observation of expanded MPC molecular areas.

Second, the voltammetric peaks of the ferrocene groups became much broader and the formal potential shifted anodically ($E^{\circ'} = +0.40$ V). Considering the suppression of the double-layer current envelope discussed above, it is rather unlikely that the decrease in ferrocene faradaic current is due to particle loss from the electrode surface. Additionally, due to the hydrophobic nature of the nanoparticles, it is energetically unfavorable that the particles would desorb from the electrode surface into the aqueous solution. Also, the peak potential splitting appears to be virtually unchanged, suggesting a thermodynamic rather than a kinetic effect. In earlier studies involving self-assembled monolayers of ferrocene-terminated alkanethiols with coadsorbed electroinactive ω -functionalized n -alkanethiol derivatives,^{10,11} it was found that, in aqueous electrolyte solutions, the formal potential of the ferrocene moiety also shifted anodically when the ω -terminal groups of the coadsorbates became less polar. This observation was interpreted on the basis of the combined effects of local ion solvation and double-layer potential distribution.^{10,11,13} These effects might also account for the present observations with the LB particle layers where the enhanced hydrophobic interaction resulting from the structural rearrangements leads to more difficult penetration for electrolyte ion for charge compensation. The broad voltammetric peak widths might reflect the wide spatial distribution of ferrocene sites on the electrode surface¹³ due to the three-dimensional nature of the nanoparticle cores, suggesting that after the surface structural reorganization the particles became less mobile.

Similar dynamic reorganizations were also observed with multilayer structures (not shown); however, the ferrocene voltammetric currents decreased to a much less extent with more MPC layers. This might be understood in terms of the decrease in MPC molecular mobility,

(16) In another study where the ω -ferrocenated particles were cross-linked at the air-water interface by rigid dithiol linkers prior to deposition onto the electrode surface,⁷ an additional pair of voltammetric peaks were found at a more positive potential position; however, the voltammetric responses were very stable. These observations were consistent with the argument of molecular mobility and consequential interfacial structural dynamics.

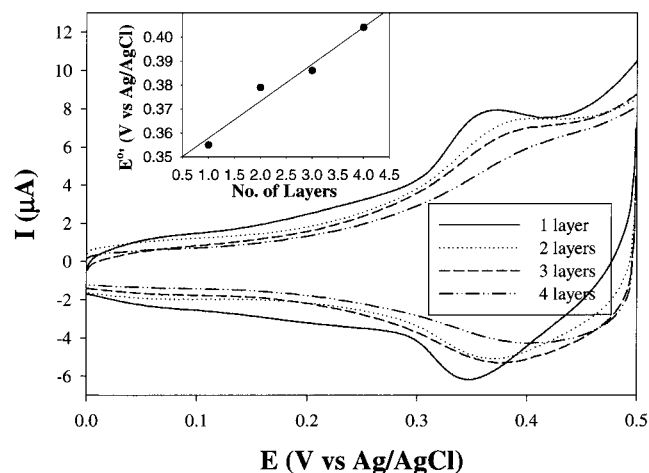


Figure 5. Cyclic voltammograms of freshly deposited C8FcAu MPC thin films of varied layers in 0.10 M KNO₃. Potential sweep rate 100 mV/s. Inset shows the variation of the formal potential of the ferrocene moiety with the number of MPC layers. Line is for eye-guiding only.

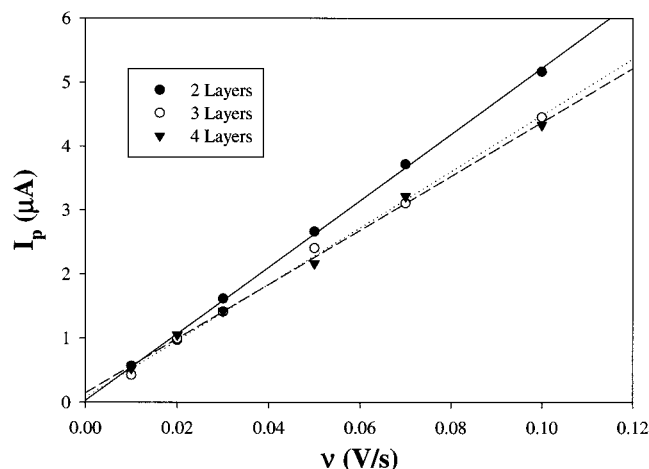


Figure 6. Variation of ferrocene faradaic currents with potential sweep rates for the varied layers of C8FcAu MPC LB thin films. Experimental conditions are the same as in Figure 5. Symbols are experimental data, and lines are the corresponding linear regressions.

especially for those buried underneath the topmost layer, based on the above speculation of interfacial structural dynamics.¹⁶

Multilayer Structures. Electrochemistry of the C8FcAu MPC multilayers shows additional unusual characters. Figure 5 depicts the cyclic voltammograms of varied layers of C8FcAu MPCs freshly deposited onto a gold thin film electrode. First, one can see that the double-layer charging current within the potential range of 0 to +0.5 V decreases with the deposition of additional MPC layers, consistent with the presence of more organically functionalized MPC molecules onto the electrode surface (vide ante). However, surprisingly, the voltammetric current due to the ferrocene moieties does not increase proportionally with the number of MPC layers, which is rather counterintuitive. While the ferrocene faradaic currents increase linearly with potential sweep rates with varied layers of C8FcAu MPCs (Figure 6), again, consistent with surface-confined systems, the slopes (S) normalized to that with an MPC monolayer (Figure 4) are $S_1:S_2:S_3:S_4 = 1:1.87:1.59:1.52$ with the subscripts referring to the number of MPC layers. This is drastically smaller than the theoretical value of $S_1:S_2:S_3:S_4 = 1:2:3:4$, which is anticipated from

the aforementioned optical measurements (Figure 2) by assuming that all ferrocene sites are active and accessible. This is in great contrast to colloidal multilayers fabricated by alternated-dipping self-assembling method with electroactive species incorporated in between the particle layers,^{17,18} where the voltammetric currents due to the faradaic processes increase linearly with the number of particle layers, indicating that all sites are accessible in the electron-transfer reactions and the porous nature of the resulting colloidal thin films. The discrepancy observed here suggests that in the LB thin films of nanoparticles, due to ligand intercalation, some ferrocene sites are buried within a hydrophobic environment which creates a large energetic barrier for charge transfer as well as charge compensation.¹³ In other words, the film behaves less conductive with more MPC layers, resulting in the decrease of accessible ferrocene sites and hence smaller voltammetric currents (Figures 5 and 6). This might also account, at least in part, for the anodic shift of the formal potential of the ferrocene moieties with more MPC layers (Figure 5, inset), where an overpotential of 15 mV is found with each additional layer of MPC molecules.¹⁹

It should be noted that, of these active ferrocene sites, their peak splittings remain very small (<40 mV), again indicating that the effect of the local environmental variation is reflected thermodynamically rather than kinetically, as mentioned earlier.

Concluding Remarks

Using the electroactive ferrocene moieties as the molecular probes, electrochemical investigations were carried out to investigate the interfacial dynamics of nanoparticle Langmuir–Blodgett thin film. The deposition of nanoparticle molecules onto the substrate surface was quite successful only in the first few layers as characterized by optical absorption measurements. It was found that in the nanoparticle monolayers the molecular mobility due to relatively weak interparticle interactions led to the potential-induced reorganization of the particle molecules, reflected in a decrease in the electrode double-layer charging current and the surprising suppression of the faradaic currents of the ferrocene moieties. With the deposition of additional nanoparticle layers, the particle thin films became less conductive, leading to the anodic shift of the ferrocene formal potential as well as the drastic decrease in ferrocene faradaic currents.

Acknowledgment. The author gratefully acknowledges the following agencies for their generous financial support: the National Science Foundation (CAREER Award), the Office of Naval Research, the Petroleum Research Fund, administered by the American Chemical Society, the Illinois Department of Commerce and Community Affairs, and SIU Materials Technology Center. S.C. is a Cottrell Scholar of Research Corporation.

Supporting Information Available: Differential pulse voltammogram (DPV) of four LB layers of ferrocenated gold nanoparticles in 0.10 M KNO₃. This material is available free of charge via the Internet at <http://pubs.acs.org>.

LA0107042

(17) Shipway, A. N.; Lahav, M.; Willner, I. *Adv. Mater.* **2000**, *12*, 993.

(18) Gittins, D. I.; Bethell, D.; Nichols, R. J.; Schiffrin, D. J. *Adv. Mater.* **1999**, *11*, 737.

(19) In the case of four layers of gold nanoclusters, the ferrocene peak potential was determined by differential pulse voltammetry (DPV). Please see the Supporting Information for details. Also, in a dropcast thick film (~μm) of the same ω-ferrocenated nanoparticles, the formal potential of the ferrocene moieties was found at an even more positive position, +0.45 V.